Identification and Control of A Piezoelectric Patch Actuator

MOHD NAZMIN MASLAN, M. MAILAH AND I.Z.M. DARUS
Department of System Dynamics and Control
Faculty of Mechanical Engineering
Universiti Teknologi Malaysia
81310 UTM Johor Bahru, Johor
MALAYSIA
irnazminm@gmail.com

Abstract: - This paper focuses on determining the transfer function (TF) of a highly nonlinear and hysteretic piezoelectric actuator and its inverse. A system identification (SI) technique was employed based on the direct measurements of the input-output data from a patch type piezoelectric actuator mounted on a suitably designed platform equipped with appropriate instrumentations. Eventually, the actuator TF models were approximated through a rigorous analytical procedure. Verification and validation of the results are performed to ensure that the transfer functions obtained are practically viable and implementable. An illustrative case study involving the control of the identified piezo actuator using closed-loop control methods employing a conventional proportional-integral-derivative (PID) controller and PID with active force control (PIDAFC). The outcome of the study clearly indicates the effectiveness of the proposed schemes.

Key-Words: - Hysteretic behaviour, piezoelectric patch actuator; transfer function, system identification, active force control

1 Introduction

Actuators incorporating smart materials are competitive choices for micro applications, but they are difficult to control because of their inherent nonlinearity and hysteresis [1]. Smart material devices in the form of piezoelectric actuators are quite common and obvious choices due to their highly desirable features in actuating mechanisms in multitude of emerging nano and bio technologies. As an example, piezo actuator is used in atomic force microscopy to image and manipulate samples at the nanoscale and also a wide range of mechatronic applications like fuel injection to the field of smart structures for micro positioning or noise and vibration suppression [2]. The actuator works on the principle of the piezo material in the actuator changes its dimension (e.g., displacement) in response to the applied voltage. This property can be used to generate motion or force in electromechanical devices and micro machines [3]. However, their highly nonlinear hysteretical stimulus-response characteristic fundamentally limits the accuracy of the actuators. A popular approach in the control of smart materials is to linearise the system by incorporating the inverse of the actuator model before the actuator. If the model can be inverted, the system can be linearised. In [4], Tan and Baras demonstrated that the actuator is linearised by an inverse model and optimal control is used to provide robust stability for the linearised system. A standards committee of the IEEE has published a description of the behaviour of piezoelectric ceramic element in terms of linearised constitutive relations. In other words, it is generally meant to describe the linear modelling of piezoceramics [5]. System identification (SI) technique has been used for the purpose of building mathematical model of dynamical system based on observed data and may provide a useful tool to study the behaviour of the piezo actuators, given the adverse and complex conditions pertaining to the dynamic motion of their internal structures. If there is no a priori knowledge available, then the structure realization might be done by a trial-and-error method [6]. The main focus in SI is on the parameter identification process. Well developed techniques such as least-square, instrumental variable and maximum likelihood exist for parameters estimation of models. However, these techniques often fail in the search for the global optimum if the search space is not differentiable or linear in the parameters [7]. The research works on the identification of the piezoelectric actuator models found in the literature are very sparse and limited. Most researchers report on the hysteretic aspect of the actuators without due consideration to other dynamics influence [1]. An identification technique applied to general actuator with hysteresis is given in [8] in which a relay feedback mechanism is employed. Sung and Lee present a method to identify piezo actuator model considering only the hysteresis aspect with PID element in the overall system [9].

In this paper, the transfer function of a patch type piezoelectric actuator and its inverse are determined through the SI technique. A case study is later presented to verify the results based on a vibration control application employing two types of closed-loop feedback control schemes, namely, the PID and PIDAFC).

2 Piezoelectric Patch Actuator

The piezoelectric patch transducer can be seen in Fig. 1. When the module is glued to a substrate, it effectively transfers force over the whole surface. The piezoceramic response to a change of the electric field is extremely fast. Vibrations in the kilohertz range can be produced. Different excitation voltages are required and different contraction amounts possible, depends on the ceramic type and dimensions. The correlation between displacement and applied voltage is not linear.

Fig. 1: PI P-876 piezoelectric patch actuators [10].

Table 1 presents the available features in the patch actuator tested.

Table 1: Specifications for the patch actuator

Parameters	Values
Dimensions L x W x T	61.0 x 35.0 x 0.4 mm
Mass	2.1 g
Active area	15 cm^2
Operating voltage	-50 to + 200 V
Free lateral contraction, S_o	400 µm/m
Lateral contraction / Voltage	1.6 (µm/m)/V
Bending radius	12 mm
Blocking force, F_B	90 N
Electrical capacitance	150 nF ±20%

3 System Identification

Identification is a method of measuring a system transfer function or some equivalent mathematical description from measurements of the system input and output. It provides a useful tool to study the behaviour of the piezoelectric actuator, given the adverse and complex conditions pertaining to the dynamic motion of their internal structures. The SI techniques have a wide application such as a solar-heated house, a military aircraft, electronic control unit (ECU) on vehicle engine and others [11]. The objective of SI is to find the exact or approximate models of dynamic system based on knowledge of the observed input and output data [12]. Fig. 2 shows a typical procedure and steps in SI.

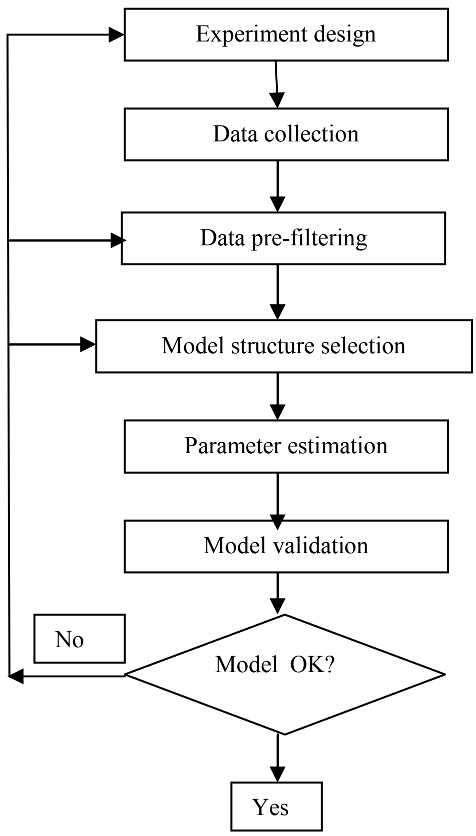

Fig. 2: Procedure of system identification technique

Consider a discrete-time (D-T) system in the form:

$$y(k) = \frac{b_1 z^{-1} + b_2 z^{-2} + \ldots + b_m z^{-m}}{1 + a_1 z^{-1} + a_2 z^{-2} + \ldots + a_n z^{-n}} u(k) \tag{1}$$

which can also be written as:

$$y(k) + a_1 y(k-1) + a_2 y(k-2) + \ldots + a_n y(k-n) \\ = b_1 u(k-1) + b_2 u(k-2) + \ldots + b_m u(k-m) \tag{2a}$$

Eq. (1) is known as the D-T transfer function. The relevant parameters can be estimated using the RLS algorithm by first transforming Eq. (2a) into a regression equation as follows:

$$y(k) = \begin{bmatrix} y(k-1) & \cdots & y(k-n) & u(k) & \cdots & u(k-m) \end{bmatrix} \begin{bmatrix} a_1 \\ \vdots \\ a_n \\ b_1 \\ \vdots \\ b_m \end{bmatrix} \tag{2b}$$

The regression in Eq. (2b) is then used in the RLS algorithm.

4 Experimental Setup and Model Identification

The experimental setup for data capturing is illustrated in the Fig. 3.

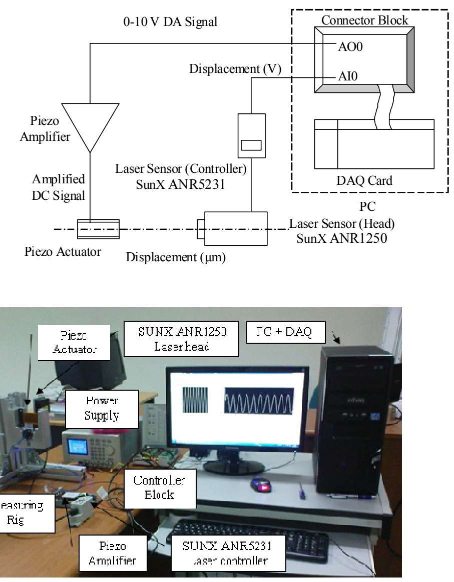

Fig.3: Experimental setup

All data capturing experiments were assessed using a laser sensor and fixed with a module jig to measure the displacement signal. The displacement signals were recorded via a personal computer (PC) at a sampling rate of 1 kHz using a 16-bit PCI Data Acquisition Card (DAQ). Data processing and routines analysis were performed using LabVIEW software. The program has been designed to automatically terminate the data collection after 10 seconds. A voltage input of 10 volt 10 Hz triangle-wave is supplied via the DAQ. This experiment is done for the actuator with its set of amplifiers that will amplify the voltage to 60 V. A series of voltages were applied to the piezo actuator which enable it to freely displace its active element at its free end with the other end fixed. Meanwhile, a low frequency (10 Hz) input waveform was used in the parameter identification to reduce the dynamic effect, which stems from the dynamics of the actuator itself. The other section of the software application is through the use of MATLAB as the main programming environment for executing the SI command lines. A MATLAB program has been created based on the RLS using ARX model. Once the transfer function model has been determined, the result shall be verified and validated via modelling and simulation using MATLAB/Simulink.

For the purpose of SI, a general problem of piezoelectric behaviour is hysteretic characteristic demonstrated between the voltage and displacement as previously shown. Prior to the displacement control of the actuator, it is essential to perform the model reduction. According to Sung and Lee, if the input voltage *u* is applied to piezoelectric actuator, the output displacement *y* will be generated, and their relation can be linearised as a second-order linear dynamic system [9]. In this section, the direct transfer function is to be determined for the given piezo actuator. The relationship between voltage *u* and displacement *y* is given in Fig. 4.

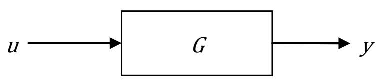

Fig. 4: Block diagram for direct transfer function

For a continuous-time system, *G* relates the *Laplace* transforms of the input *U(s)* and output *Y(s)*, as follows:

$$G(s) = \frac{Y(s)}{U(s)} \tag{3}$$

4.1 Direct TF of Patch Actuator

Fig. 5 shows the endpoint displacement of patch actuator to a 250 volt 10 Hz triangle-wave voltage input.

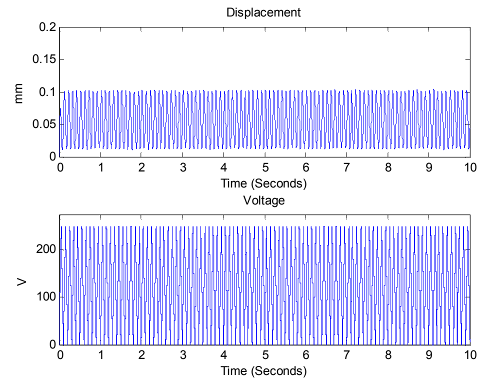

Fig.5: Endpoint displacement of patch actuator for direct TF

In the following section, the inverse transfer function is to be determined for the given piezo actuator. The main variation from the past method is switching both the input and output variables. The relationship between displacement *y* and voltage *u* is as shown in Fig. 6.

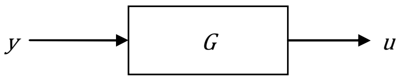

Fig. 6: Block diagram for inverse transfer function

For a continuous-time system, G^{-1} relates the *Laplace* transform of the input *U(s)* and output *Y(s)*, as follows:

$$G^{-1}(s) = \frac{Y(s)}{U(s)} \tag{4}$$

4.2 Inverse TF of Patch Actuator

Fig. 7 shows the trend of the endpoint voltage to an input displacement of the patch actuator.

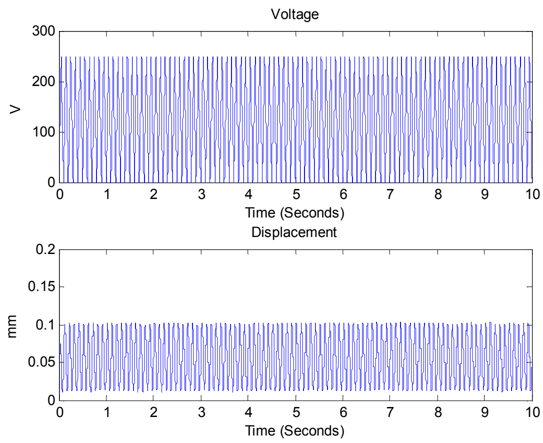

Fig.7: Endpoint displacement of the patch actuator for inverse TF

Figs. 8 and 9 show the validation results obtained from the actuator for both direct and inverse transfer functions.

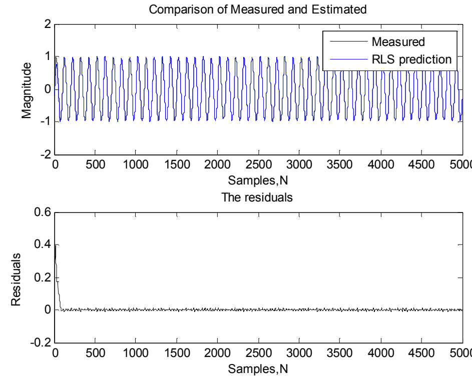

(a)

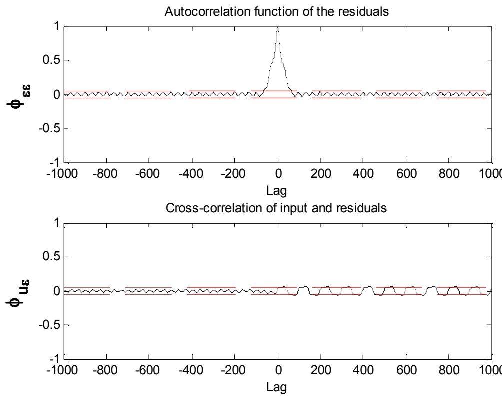

(b)

Fig.8: Validation results of the patch actuator for direct TF.

The model output plot uses input validation data as input to the model and plots the simulated output on top of the output validation data. Figs. 8(a) and 9(a) shows agreement between the RLS prediction and the measured output in the validation data. The error signal or residuals can be observed that the prediction significantly drops the error.

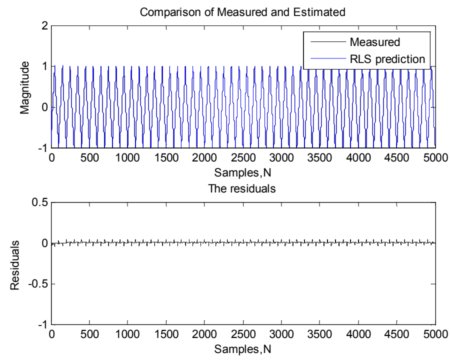

(a)

ISBN: 978-1-61804-094-7

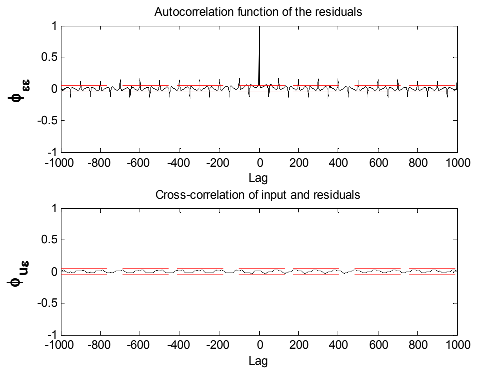

(b)

Fig. 9: Validation results of patch actuator for inverse TF

Besides the model output plot, a model can be validated by checking the behaviour of its residuals. The horizontal axis is the number of lags, which is the time difference (in samples) between the signals at which the correlation is estimated. The 95% confidence intervals for these values are also computed and shown as a region inside the red lines. The top axes show the autocorrelation of residuals for the output (whiteness test). It determines whether or not the error signal is a white noise. A good model should have a residual auto-correlation function within the confidence interval, indicating that the residuals are uncorrelated (certain error is white noise). For the given actuator, the residuals appear to be uncorrelated as shown in Figs. 8(b) and 9(b) as it falls within the confidence bounds.

Simultaneously, the bottom axes show the cross-correlation of the residuals with the input (independence test). A good model should have residuals uncorrelated with past inputs (independent with each other). If not at lag k, it implies that the contribution to the output $y(t)$ that originates from the input $u(t-k)$ is not properly described by the model. Referring to the figures again, i.e., Figs. 8(b) and 9(b), there is no correlation between the residuals and the inputs. The whiteness test for the RLS prediction shows that the residuals are uncorrelated, and the independence test shows no correlation between the residuals and the inputs. Thus, the RLS prediction method produces a good model. Both direct and inverse models produce a mean square error (mse) of 6.2686 X 10^{-4} and 2.3511 X 10^{-4}, respectively. The experimental results and the SI approach give the following direct transfer function for the patch actuator:

$$G(s) = \frac{0.03747s^2 - 0.07066s + 0.03319}{0.4882s^2 - 1.492s + 0.0039} \quad (5)$$

Meanwhile, the corresponding inverse transfer function model is found to be:

$$G^{-1}(s) = \frac{-0.04314s^2 + 0.07153s - 0.0284}{0.4795s^2 - 1.487s - 0.0071} \quad (6)$$

5 Case Study: Control Application

This section presents the simulation works for a position control of the piezoelectric patch actuator. The simulation was performed using MATLAB and Simulink. To test the model in an advanced non-linear control systems, parameters for the dynamic system was taken from a research [13] done using the same type of patch actuator. The objective of the study is to suppress the unwanted vibration of a simple 1-DOF system. Extensive research has been done to highlight the robustness of the active force control (AFC) scheme [14-16] applied to various dynamical systems. The system typically remains stable, robust and efficient although the system is operated at high speed and exposed to various forms of external disturbances. The conventional PID controller was first simulated followed by a PIDAFC scheme. Assuming that all the gains of the PID and AFC systems have been appropriately obtained using a typical heuristic method, the transfer function models (direct and inverse) of the patch actuator determined earlier are directly incorporated into the relevant actuator blocks and then the scheme is tested against a unit step input and a vibratory excitation. Fig. 10 shows the block diagram of the control system with a switch incorporated to activate between the PID and PIDAFC control modes.

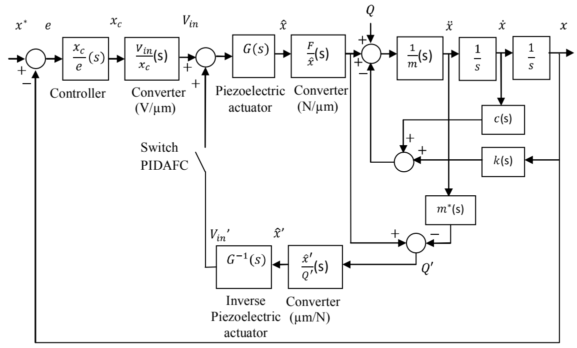

Fig. 10: Schematic of the PIDAFC scheme

The desired input is set at 1 as in 1 µm. A sinusoidal disturbance with amplitude of 10 and frequency of 10 Hz was applied to the dynamic system. The dynamic response of the system during 1 s was studied. A variable sampling time at 0.02 maximum step size was chosen in the simulation study. Finally, the output response of the simulated control method is plotted to describe the differences in performance under similar operating and loading conditions as shown in Fig. 11. The solid line is the result attributed to the PID control while the dashed line is the one generated by the PID with AFC scheme (PIDAFC). From the plot, it is obvious that both control methods produce comparable performance with the PIDAFC scheme showing a slightly better result (without fluctuations at the initial stage).

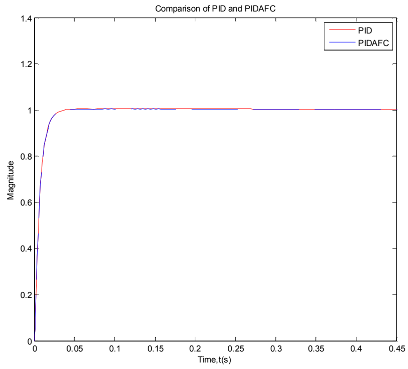

Fig. 11 Comparison of the tracking control performance.

6 Conclusion

The transfer functions of a piezo patch actuator and its inverse have been successfully derived and validated using the proposed identification and control techniques. It is evident that the PIDAFC scheme manages to suppress effectively the unwanted vibration affecting the one-DOF system through the incorporation of the newly-derived direct and inverse transfer functions of the actuator.

Acknowledgements

The authors would like to acknowledge the Malaysian Ministry of Higher Education (MOHE) and the Universiti Teknologi Malaysia for their full support of this research through a Fundamental Research Grant Scheme (Vote No.: 4F377).

References:

[1] H.T. Banks, A.J. Kurdila, G. Webb, Identification of Hysteretic Control Influence Operators Representing Smart Actuators Part I: Formulation, *Mathematical Problems in Engineering,* Vol. 3, 1997, pp. 287-328.

[2] Y. Wu, S. Culter, Z. Qingze, G. Pannozzo, K. Leang, S. Devasia, Modelling and Control of Smart Actuators: Integrating Nano/Bio technology into the ME Curriculum, *Transactions of American Society for Engineering Education,* 2007, AC 2008-814.

[3] S. Valadkhan, K. Morris, A. Khajepour, Modeling Robust Control of Smart Material-based Actuators, *Recent Advances in Learning and Control,* Vol. 371, 2008, pp. 249-262.

[4] X. Tan, J.S. Baras, Modeling and Control of Hysteresis in Magnetostrictive Actuators, *Automatica,* Vol. 40, 2004, pp. 1469-1480.

[5] IEEE, An American National Standard, in *IEEE Standard on Piezoelectricity, Standards Committee of IEEE Ultrasonics, Ferroelectrics, and Frequency Control Society,* The Institution of Electrical and Electronics Engineers, ANSI/IEEE Std, 1987, pp. 176-1987.

[6] W. Levine, *The Control Handbook.*: CRC Press, 1995.

[7] M.A. Hossain, M.O. Tokhi, A.J. Chipperfield, M.J. Baxter, C.M. Fonseca, N.V. Dakev, Adaptive Active Vibration Control using Genetic Algorithms, Procs. of 1st International Conference on Genetic Algorithms in Engineering Systems: Innovations and Applications, pp. 175-180, 1995.

[8] Y.C. Cheng, C.C. Yu, Relay Feedback Identification for Actuators with Hysteresis, *Industrial & Engineering Chemistry Research,* Vol. 39, 2000, pp. 4239-4249.

[9] B.J. Sung, E.W. Lee, I.S. Kim, Displacement Control of Piezoelectric Actuator using the PID Controller and System Identification Method, Procs. of International Conference on Power System Technology, India, 2008, pp. 1-7.

[10] Physik Instrumente, Piezo Nano Positioning, GmbH & Co. KG, 2008.

[11] L. Ljung, *System Identification: Theory for the User*, 2nd Edition. Upper Saddle River, NJ Prentice Hall PTR 1999.

[12] P.E. Wellstead, M.B. Zarrop, *Self-Tuning Systems: Control and Signal Processing*, John Wiley & Sons Ltd., 1991.

[13] S. Kazi, Development of Smart Glove with Intelligent Tremor Control using Piezo-Electric Actuator, PhD Thesis, UTM, 2011.

[14] J.R. Hewit, J.S. Burdess, Fast Dynamics Decoupled Control for Robotics using Active Force Control, *Mechanism and Machine Theory,* Vol. 16, No. 5, 1981, pp. 535-542.

[15] M. Mailah, S. Meeran, J.R. Hewit, Active Force Control Applied to a Rigid Robot Arm, *Jurnal Mekanikal,* 1996, pp. 52 – 68.

[16] A.R. Tavakolpour, M. Mailah, I.Z.M. Darus, Vibration Control of a Flexible Thin Plate Using Active Force Control Strategy, Procs. of the 2nd International Conference on Instrumentation and Mechatronics, Malaysia, 2009.